CrossMark

RESEARCH PAPER

Relationship between penetration and porosity in horizontal fillet welding by a new process "hybrid tandem MAG welding process"

Yimin Yuan[1] · Kei Yamazaki[1] · Reiichi Suzuki[1]

Abstract In the shipbuilding and bridge construction industries, shop primer paint is coated to the surface of steel plates in order to protect them from rusting during a long fabrication period. However, when arc welding is applied to the primer-coated plates, the arc heat may decompose and vaporize the coating. Then, the generated gas will be enclosed in the weld metal during the solidification process, causing the porosity defects, such as blowholes and the pits. In this study, the effects of penetration depth and non-penetrated joint root length on the generation of blowholes were clarified with various welding parameters. A new horizontal fillet welding process called 'hybrid tandem MAG (HTM)' was developed, a combination of a solid wire for the leading electrode and a flux-cored wire for the trailing electrode. The process features deep penetration and excellent porosity resistance. In order to reduce porosity in the fillet welding of primer-coated steel plate, it was found that the following measures are effective: (a) increasing the penetration depth and (b) decreasing the non-penetrated joint root length. The reduction of porosity by increasing the penetration depth is achieved by the formation of consistent ejection passage for vaporized gas. The phenomena mentioned above were verified by observing the interior of the weld pool directly by using an X-ray video camera. It is effective to reduce the leading electrode torch angle and to use a combination of high current and low voltage to create a buried arc to realize these measures. The MAG (HTM) procedure reduced the porosity formation to one tenth of that produced with the conventional tandem MAG process even at travel speeds up to 1600 mm/min.

1 Introduction

In the shipbuilding and bridge construction industries, steel plates are coated with shop primer paint to protect their surfaces from rusting during the fabrication period for block structures. However, when arc welding is carried out on the primer-coated plates, the arc heat can decompose and vaporize the coating, thus so generating gases [1], which are then enclosed in the weld metal during the solidification process, thereby causing blowholes and pits (The term pits is used here to describe surface breaking porosity) (Fig. 1).

Several means have previously been used to improve the porosity resistance in the welding of primer-coated plates, which include (1) the modification of primer-paint composition and (2) the development of new filler metals by modifying slag chemistry [1–4]. Nevertheless, the occurrence of porosity has not been reduced sufficiently, and thus, further improvement is currently required. The present research focused on clarifying mechanism of porosity generating blowholes and on the means of discharging generated gases into the air at an early stage of the gas generation process. In this report, the effects of penetration depth and non-penetrated joint root length on the generation of blowholes were clarified with various welding parameters, and a new horizontal fillet welding process called 'hybrid tandem MAG (hereafter: HTM)' was
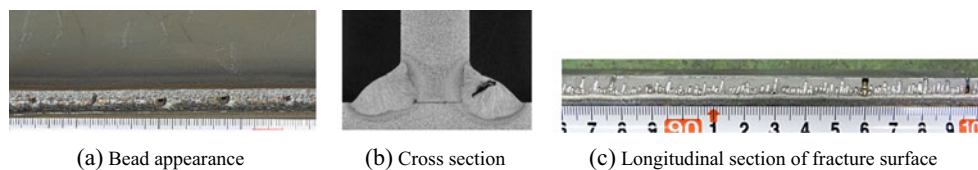
✉ Yimin Yuan
  yuan.yimin@kobelco.com

[1] Welding Business, Kobe Steel, Ltd., 100-1 Miyamae, Fujisawa, Kanagawa 251-8551, Japan

Springer

Fig. 1 Problems of horizontal fillet welding on shop-primer-coated steel plates

(a) Bead appearance   (b) Cross section   (c) Longitudinal section of fracture surface

developed by reflecting on this knowledge, which uses a combination of a solid wire for the leading electrode (hereafter: L-eletrode) and a flux-cored wire (hereafter: FCW) for the trailing electrode (hereafter: T-eletrode) featured deep penetration and excellent porosity resistance.

2 Conventional tandem MAG welding of primer-coated steel plates

By using conventional single and tandem welding processes, horizontal fillet welds were produced to obtain a leg length of approximately 7 mm. The welding conditions are shown in Table 1. Welded coupons were investigated by the radiographic test (hereafter: RT) as shown in Fig. 2. Figure 3 shows the test results of porosity occurrence. With conventional single and tandem processes, a large amount of porosity was generated inside the fillet weld beads, the initiation sites of which were aligned along the root of the fillet joint. In addition, it was also clear that the porosity grew larger in the second bead because the paths, for discharging the gases generated from the primer coating, were blocked behind the first bead. These results suggested that the gases vaporized from the primer coating and moved out of the fillet joint root, to enter the weld pool.
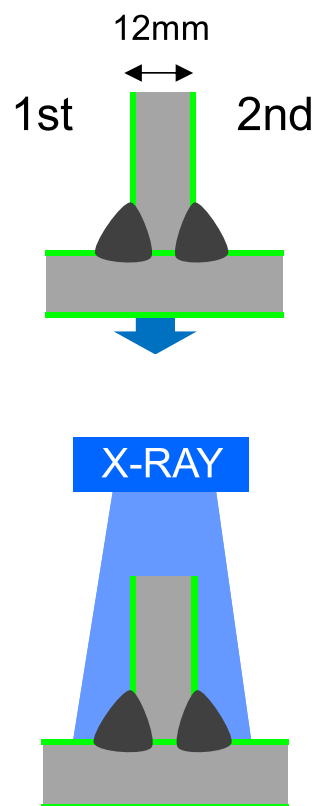
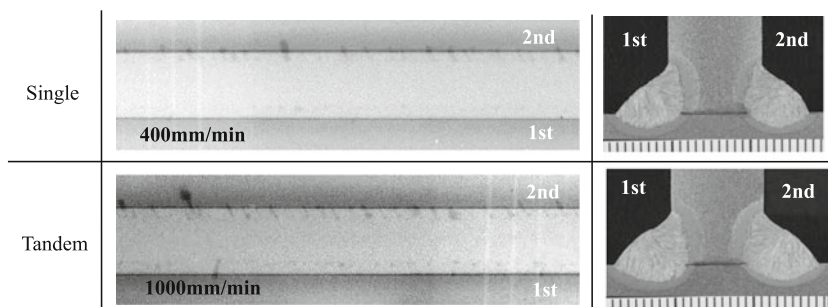## 3 Consideration and examination on how to reduce porosity

Earlier research on the welding of galvanized steel sheets demonstrated that, by adjusting the shielding gas composition, pulse waveform, and welding wire chemistry, the arc could be made strong enough to dig deeply into the weld pool, thereby effectively ejecting the majority of zinc vapour from the weld pool beneath the arc reducing porosity [5–7]. In the present research, the authors considered the porosity generation mechanism in the welding of primer-coated steel plates to be the same as that in the welding of galvanized steel sheets and based a porosity reduction method, suitable for horizontal fillet welding.

With the conventional welding process, the vaporized primer gas probably generates at the fillet joint root and enters the weld pool. This gas, then, begins to expand from the root to form blowholes and pits. The authors considered that if the fillet joint root could be fused completely, eventually

Table 1 Conventional welding condition

Base metal	Carbon steel, SM490A, 12 mm (shop primer: 30 μm)		
Joint type	Horizontal fillet		
Shielding gas	100 % CO_2		
Process	Single	Tandem	
Electrode		Lead	Trail
Wire	FCW, 1.4 mm diameter	FCW, 1.6 mm diameter	FCW, 1.6 mm diameter
Tip to work distance	25 mm	25 mm	25 mm
Torch angle θ_1	45°	45°	45°
Torch angle θ_2	0°	Backhand 7°	Forehand 7°
Wire feed rate	12.0 m/min	12.0 m/min	7.0 m/min
Current-voltage	330 A–34 V	430 A–32 V	320 A–30 V
Welding speed	400 mm/min	1000 mm/min	
L-T distance		25 mm	

12mm

1st   2nd

X-RAY
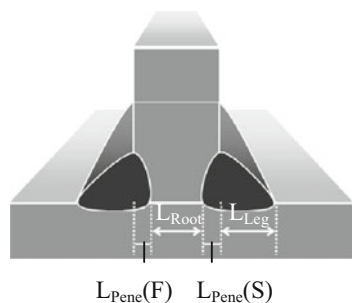
Fig. 2 RT observation method

Fig. 3 RT result and penetration with conventional process

Table 2 Test welding condition

Base metal	Carbon steel, SM490A, 12 mm (shop primer: 30 μm)	
Joint type	Horizontal fillet	
Shielding gas	100 % CO_2	
Electrode	Lead	Trail
Wire	Solid Wire, 1.6 mm diameter	FCW, 1.4 mm diameter
Tip to work distance	13 mm	25 mm
Torch angle θ_1	5°–45°	45°
Torch angle θ_2	Backhand 7°	Forehand 7°
Wire feed rate	5.5–11.0 m/min	10.0–17.0 m/min
Current	350–550 A	300 A–370 V
Voltage	20–35 V	30–37 V
Welding speed	1000 mm/min	
L-T distance	30 mm	

eliminating a non-penetrated joint root, all the vaporized primer gas could be released from the weld pool, thereby preventing the occurrence of porosity. In order to realize this, consistent deep penetration was considered to be important. Based on this consideration, the fillet welding method, suitable for obtaining consistent deep penetration, was first examined in the present study. Subsequently, with varied welding parameters, the effects of joint penetration depths and non-penetrated joint roots on the occurrence of blowholes were
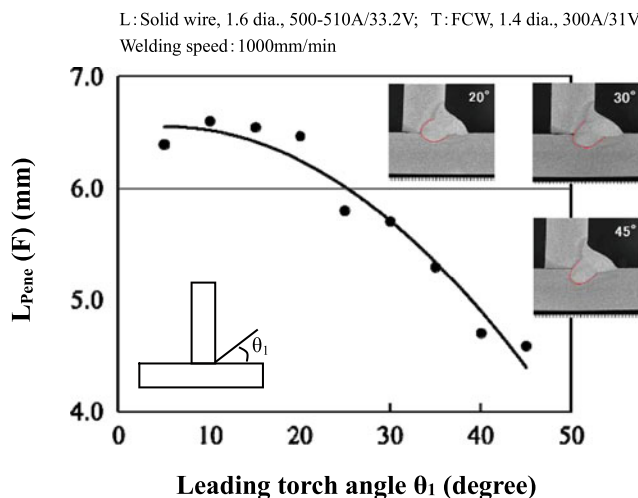
clarified. Finally, the porosity generation mechanism was verified by using an X-ray transmission high-speed video camera.

4 Effects of welding parameters on penetration depth

The authors' previous research on the tandem welding process with multiple electrodes clarified that the L-electrode was governed by joint penetration depth [8, 9]. Therefore, in the present study, the effects of L-electrode torch angle, welding current, and arc voltage on joint penetration were investigated; the welding conditions are shown in Table 2.
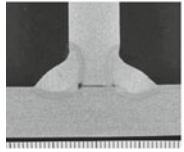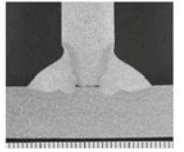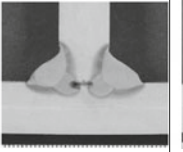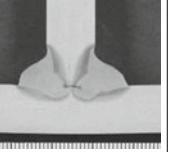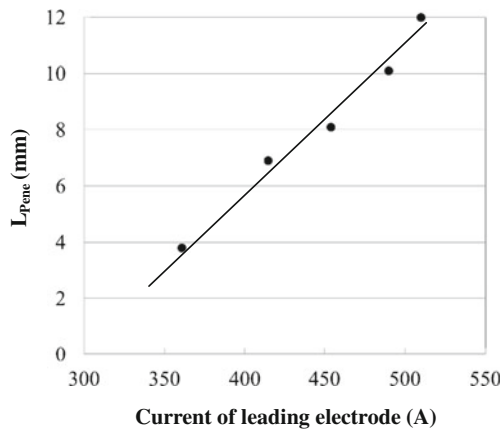
4.1 Effect of torch angle on penetration depth

In this study, joint penetration depth of both sides (L_{Pene}), non-penetrated joint root (L_{Root}), and leg length (L_{Leg}) were defined, as shown in Fig. 4. The penetration direction was considered variable to a large extent, according to the torch angle of the L-electrode. Taking this into consideration, only the torch angle θ_1 of the L-electrode was varied from 5° to 45° in one-side fillet welding so as to investigate its effects on joint penetration. The metallographic results showing depth of

$L_{Pene} = L_{Pene}(F) + L_{Pene}(S)$ 【(F):First side、 (S):Second side】

Fig. 4 Definition of L_{Pene}, L_{Root}, and L_{Leg}

L：Solid wire, 1.6 dia., 500-510A/33.2V；T：FCW, 1.4 dia., 300A/31V
Welding speed：1000mm/min

Fig. 5 Relationship between leading torch angle and L_{Pene} (F)

Table 3   Comparison of penetration depth

Current of leading electrode	360A	415A	454A	480A
L_{Pene}	3.8mm	6.9mm	8.1mm	10.1mm
Cross section				

Fig. 6 Relationship between current of leading electrode and penetration depth

penetration are shown in inset macrographs in Fig. 5, which the torch angle θ_1 was fixed at 45°, 30°, and 20°, respectively. As shown with macrographs in Fig. 5, as the torch angle θ_1 was reduced from 45° to 20°, the penetration direction changed, and the first-side joint penetration depth (L_{Pene}) (F) became larger from 4.5 to 6.5 mm. In the following experiments, the torch angle θ_1 of the L-electrode was fixed at 20° to avoid problems such as the interference between the torch and the flange plate.

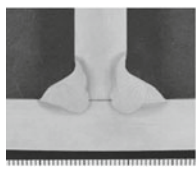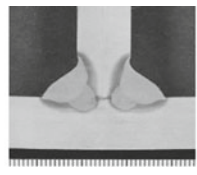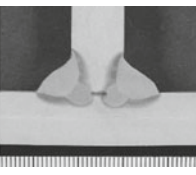### 4.2 Effect of L-electrode welding current on penetration

With the L-electrode torch angle θ_1 fixed at 20° and the L-electrode welding current changed from 350 to 520 A, horizontal fillet welds were kept at approximately 7 mm (L_{Leg}). The metallographic results showing depth of penetration are shown in Table 3 in relation to varied L-electrode welding currents, and the measurements of L_{Pene} are shown in Fig. 6 as a function of the welding currents. From these results, it is clear that L_{Pene} increased as the electric current increased.

4.3 Effect of L-electrode arc voltage on penetration

The L-electrode wire feed rate was fixed at 7, 8, and 9 m/min, respectively, and the arc voltage was changed to modify the arc mode from a buried arc to an open one in order to examine the effects of arc voltage on penetration. In this case, the T-electrode conditions were also adjusted so that L_{Leg} became approximately 7 mm.

Table 4 shows typical cross-sectional macrographs so as to observe penetration profiles at a wire feed rate of 8 m/min. Clearly, as the arc voltage decreased, the arc became more deeply buried, thereby increasing L_{Pene}. In addition, Fig. 7 shows the relationship between arc voltage and penetration at each wire feed rate. At any of these rates, the penetration tended to increase as arc voltage was reduced.

Table 4   Comparison of penetration depth

Wire feed rate	8m/min		
Current-Voltage (Leading electrode)	474A-31.6V	464A-29.1V	454A-26.3V
L_{Pene}	7.2mm	8.1mm	8.7mm
Cross section			
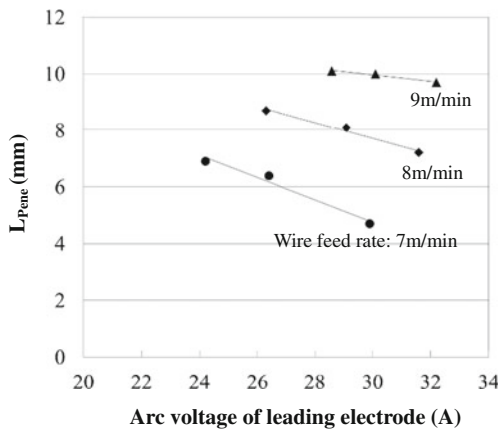
Fig. 7 Relationship between arc voltage of leading electrode and penetration depth
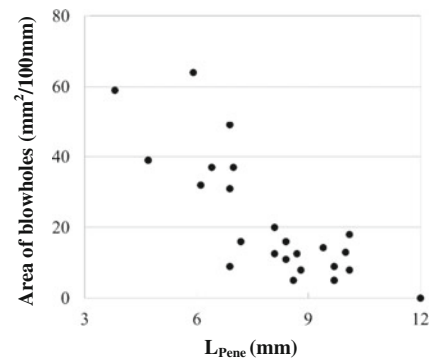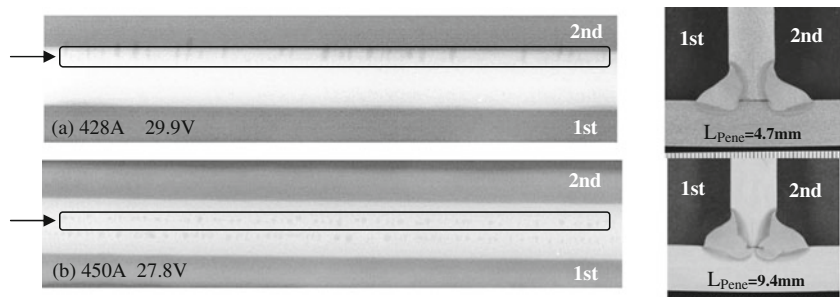
Table 5 Test welding condition

Base metal	Carbon steel, SM490A, 12 mm (shop primer: 30 µm)	
Joint type	Horizontal fillet	
Shielding gas	100 % CO_2	
Electrode	Lead	Trail
Wire	Solid Wire, 1.6 mm diameter	FCW, 1.4 mm diameter
Tip to work distance	13 mm	25 mm
Torch angle θ_1	20°	45°
Torch angle θ_2	Backhand 7°	Forehand 7°
Current	350–520 A	300A–370 V
Voltage	20–33 V	30–37 V
Welding speed	800–1400 mm/min	
L-T distance	30 mm	

5 Effects of several factors on blowhole quantity

5.1 Effect of penetration depth L_{Pene} on blowhole quantity

For assessing the amount of blowholes, horizontal fillet welds were made on the first and second sides to obtain a L_{Leg} of approximately 7 mm in the welding conditions shown in

Fig. 9 Relationship between L_{Pene} and area of blowholes

Table 5, and the welds were examined by the radiographic test (RT) as shown in Fig. 2. Subsequently, the total area of blowholes for every 100 mm of weld axis was measured on the negative film images to compare the blowhole quantity of individual test coupons. Typical RT test results are shown with photographic negative film and cross-sectional macrographs in Fig. 8, for the test coupons having a small and large L_{Pene}, respectively. In the case where L_{Pene} was approximately 4.7 mm, significant amount of porosity could be observed inside the weld bead. By contrast, in the case where L_{Pene} was 9.4 mm, the amount of porosity decreased, resulting in small blowholes, remaining in the deepest area in the weld bead.

Figure 9 shows the relationship between the penetration (L_{Pene}) and the area of blowholes. It is obvious that this area is reduced as penetration becomes deeper. This suggests that deeper penetration is advantageous for decreasing the amount of porosity. This is presumably because the vaporized primer gas is discharged more effectively beneath the arc. This is verified in Section 6 below.

5.2 Effect of non-penetrated joint root L_{Root} on blowhole quantity

In order to investigate the effect of L_{Root} on the occurrence of blowholes, horizontal fillet welding was carried out on fillet joints with various web plate thicknesses of 9, 12, and 16 mm, respectively (flange plate thickness: 12 mm) with the use of consistent welding parameters.

Fig. 8 Comparison of RT result and penetration depth

Table 6 Test welding condition

Base metal	Carbon steel, SM490A, 9–16 mm (shop primer: 30 μm)	
Joint type	Horizontal fillet joint	
Shielding gas	100 % CO_2	
Electrode	Lead	Trail
Wire	Solid Wire, 1.6 mm diameter	FCW, 1.4 mm diameter
Tip to work distance	13 mm	25 mm
Torch angle θ_1	20°	45°
Torch angle θ_2	Backhand 7°	Forehand 7°
Welding speed	1000 mm/min	
L-T distance	30 mm	

Fig. 10 Relationship between L_{Root} and area of blowholes

Subsequently, the blowhole quantity was compared by RT examination. With consistent welding parameters, L_{Pene} could be controlled uniformly, and thus, only L_{Root} could be changed. Table 6 shows the welding parameters (excluding the welding current and arc voltage), used for this comparison test. Table 7 shows the test results associated with welding current, arc voltage, and web plate thickness. Also, Fig. 10 shows the relationship between L_{Root} and the area of blowholes. In every welding condition, the area of blowholes tended to increase as L_{Root} became larger. This is probably because the source of gas generation remained in the joint root, which can cause blowholes; therefore, blowholes increased as L_{Root} becames larger.

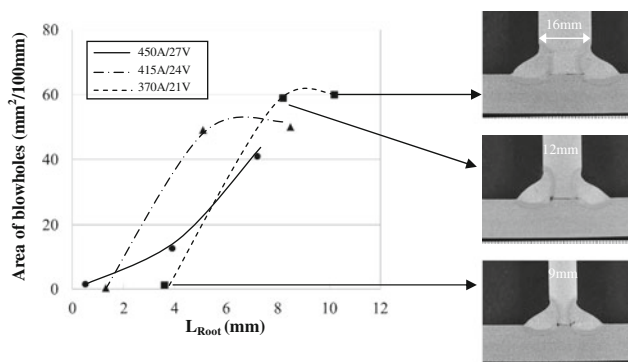### 5.3 Summary of effects of several factors on blowhole occurrence

From the abovementioned examination results, it can be determined that the following two measures control the reduction of porosity.

(1) The increase of penetration depth (L_{Pene}).
(2) The decrease of non-penetrated joint root (L_{Root}).

These two measures can be executed by using (a) higher welding currents, (b) lower arc voltages, and (c) smaller torch angles (θ_1) for the leading electrode. By combining these, a buried arc can be obtained.

6 Visualization of porosity occurrence

6.1 Observation of weld pool beneath the L-electrode arc in conventional and developed processes

To confirm the porosity formation phenomenon directly, the behaviour of blowholes in the weld pool during welding was observed at a frame rate of 500 fps by using an X-ray transmission high-speed video camera (tube voltage: 180–225 kV and tube current: 3.0–3.5 mA). In this observation test, the primer coat thickness was doubled to accelerate its adverse effect on the porosity occurrence, and lap fillet joints (with a 12-mm overlap) were used in order to obtain clear radiographs (Fig. 11). For every weld, the second-side bead was observed in the welding conditions as shown in Table 8.

The typical observation results of the behaviour of blowholes in the weld pool during welding by the conventional process are shown in Fig. 12. The primer paint gas that was vaporized at the lap joint root entered the weld pool right behind the arc and began to expand from the root, thereby becoming blowholes or pits.

Table 7 Comparison of penetration depth

Web plate (mm)	450 A–27 V		415 A–24 V		370 A–21 V	
	L_{Root} (mm)	B.H. (mm^2/100 mm)	L_{Root} (mm)	B.H. (mm^2/100 mm)	L_{Root} (mm)	B.H. (mm^2/100 mm)
9	0.5	1.5	1.3	0.2	3.6	1.2
12	3.9	12.6	5.1	49.0	8.2	59.0
16	7.2	41.0	8.5	50.0	10.2	60.0

B.H. (mm^2/100 mm): area of blowholes

Fig. 11 X-ray observation method

Fig. 12 Behaviour of blowholes in conventional welding process
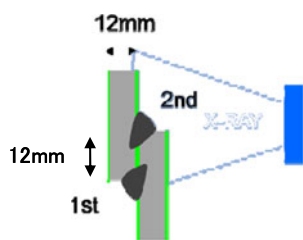
By contrast, with the developed welding process, the tip of the L-electrode was observed to be buried inside the weld pool, and its arc force deeply gouged the base metal as shown in Fig. 13. In this case, it was found that the vaporized primer gas moved out of the weld pool through a certain passage, and hence, porosity did not grow in the weld pool. In the case of complete joint penetration, even when some porosity remained in the first-side weld bead, the porosity gas was found to be discharged outside the bead by the melting effect of the opposite second-side weld penetration.

Fig. 13 Behaviour of blowholes being exhausted in developed welding process

6.2 Observation of porosity generation phenomenon in relation to penetration depth

Figure 14 shows the observation results of porosity generation in relation to penetration depth in the buried arc condition. The radiograph (a) was obtained under the welding where there was comparatively lower welding current and shallower penetration, and thus, a great deal of porosity occurred. In contrast to this, a radiograph (b) was taken in the deep penetration condition, in which the base metal was observed to be deeply gouged. As a result, a gas-releasing passage was probably formed steadily, and thus, most of the vaporized primer gas was discharged from the area beneath the arc. From these observation results, it was verified that the use of a high-current buried arc is important in order to release porosity from the weld pool.

7 Development of the hybrid tandem MAG (HTM) welding process to minimize blowhole occurrence

7.1 System configuration of HTM welding process

In order to realize the factors verified necessary through the research for the improvement of porosity resistance, the HTM welding process was developed; this configuration is shown in Fig. 15 [10]. This system consists of a 1.6-mm-diameter solid wire L-electrode and a T-electrode of 1.4-mm slag-type flux-cored wire (FCW). In addition, the L-electrode torch angle with a flange plate was set at a minimum of 20° so as to obtain deeper penetration, and the T-electrode torch angle was set at 45° to regulate the bead shape. Furthermore, the welding parameters for the L-electrode were set as such in order to obtain a high-current buried arc.

Table 8 Test welding condition

| Base metal	Carbon steel, SM490A, 12 mm (shop primer: 60 μm)			
Joint type	Lap joint			
Shielding gas	100 % CO_2			
Process	Conventional tandem		Developed tandem	
Electrode	Lead	Trail	Lead	Trail
Tip to work distance	25 mm	25 mm	13 mm	25 mm
Torch angle θ_1	45°	45°	20°	45°
Torch angle θ_2	Backhand 7°	Forehand 7°	Backhand 7°	Forehand 7°
Wire	FCW, 1.6 mm diameter	FCW, 1.6 mm diameter	Solid wire, 1.6 mm diameter	FCW, 1.4 mm diameter
Current-voltage	430 A–32 V	320 A–30 V	400~520A, 26~32 V	300~330 A, 31~33 V
Welding speed	1000~1400 mm/min			
L-T distance	25 mm		30 mm	

Fig. 14 Comparison of blowhole generation (leading electrode current: 380 and 480 A)
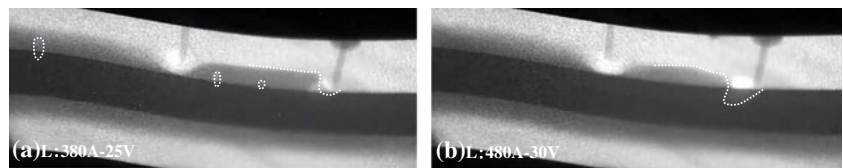
Fig. 15 Comparison of conventional tandem and hybrid tandem MAG welding processes
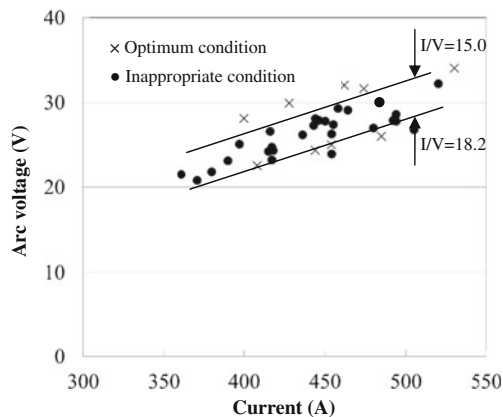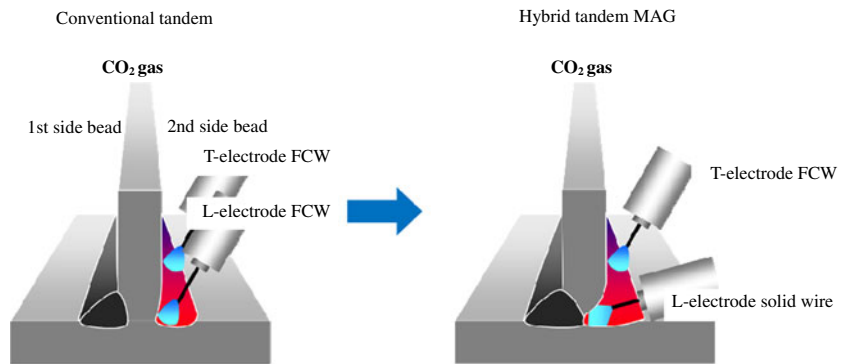
Fig. 16 Relationship between current and arc voltage of leading electrode

7.2 Optimized L-electrode welding current

As shown in Fig. 6 for the previous test results, the penetration depth (L_{Pene}) was tested in relation to the L-electrode welding current. In that test, when the L-electrode welding current was 350 A, a great deal of spatter was generated, and the penetration depth was insufficient. Also, when it was 550 A or higher, the arc force and the bulge of the weld pool between the L and T-electrodes became excessively large and unstable, thereby causing difficult normal bead formation. Based on these findings, it can be considered that the proper L-electrode welding current for the HTM process should be between 400 and 530 A.

7.3 Setting the welding current-voltage ratio

From the test data shown in Fig. 7, it is clear that arc voltage is a critical parameter for creating a buried arc, and the ratio of welding current to arc voltage (I/V ratio) has to be set in an appropriate range. When the I/V ratio is excessively large, the wire will run too much into the weld pool to maintain a stable buried arc. By contrast, when the I/V ratio is small, the arc will become open, and thus, neither little spatter can be maintained nor deep penetration can be obtained, thereby causing inferior porosity resistance. The relationship between L-electrode welding current and arc voltage is shown in Fig. 16. Clearly, the proper I/V ratio ranges from 15.0 to 18.2. Therefore, it can be considered that the proper range of this ratio for the HTM process should also be at about the same range.

7.4 Improvement of blowhole resistance

The HTM process was applied to weld the fillet joint (plate thickness: 12 mm) shown in Table 1, and the typical result is shown in Fig. 17. At the same welding speed of 1000 mm/min as that in the conventional process (Fig. 3), no porosity was observed by this process in either the first- or second-side bead. The cross sections of the fillet weld were inspected, and it was found that the HTM process exhibited complete joint penetration in contrast to the conventional single and
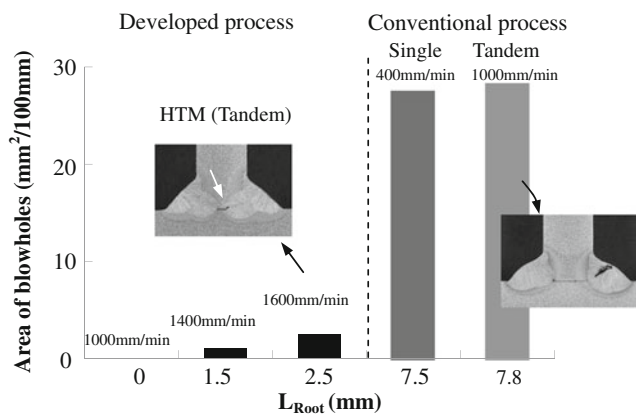
Fig. 17 RT result and penetration by HTM process
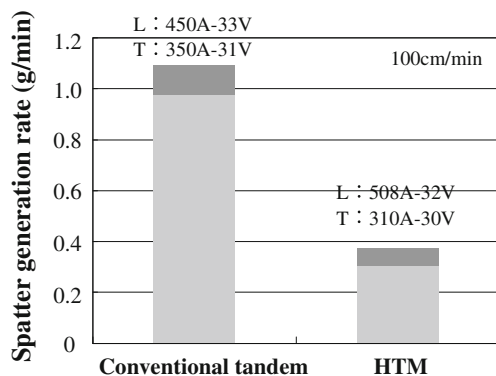
Fig. 18 Comparison of area of blowholes

Fig. 19 Comparison of spatter generation rate

tandem processes by which the non-penetrated joint root (L_{Root}) of approximately 7 mm was observed in the fillet joint root. The capability of realizing zero porosity can be explained with the observation results shown in Fig. 13., namely, in the case of complete joint penetration, even when some porosity remained at the root of the first-side weld bead, the porosity's interior gas could be discharged by the opposite second-side weld bead penetration. This is why, using the present experimental conditions that enabled complete joint penetration, porosity-free welding could be established along the entire weld length.
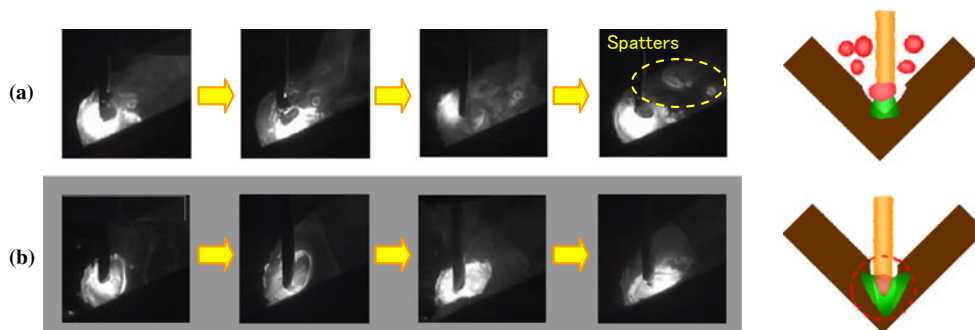
In cases in which the welding speed or plate thickness increased when using the HTM process, complete joint penetration could not be established. However, it was confirmed that porosity did not markedly increase (Fig. 18). With the conventional process, the porosity area resulted in approximately 30 mm^2/100 mm, whereas with the HTM process, the area reduced to approximately 3 mm^2/100 mm even at a high welding speed of 160 cm/min. In addition, as obvious in the cross-sectional macrograph in the use of the conventional process, the blowholes grew larger especially when reaching the bead surface. Therefore, the abrasive blasting of the weld bead surface is a liable cause porosity to appear as a pit. By contrast, with the HTM process, even when some porosity may appear, it will grow no further than the root area, and thus, the pit problem can be lessened.

7.5 Other advantages

7.5.1 Low spatter

Figure 19 shows comparison of the spatter generation rates in conventional and developed welding processes. Clearly, the HTM process can reduce the spatter generation rate by 66 % as compared to the conventional tandem process. To investigate the reason for this, the metal transfer mode was observed. In order to make it easier to observe the metal transfer by a high-speed camera, flat fillet welding was conducted. Generally, in high-current CO_2 arc welding, the arc force, strengthened by arc constriction, pushes up the molten droplet where upon, it rotates, scattering a great deal of spatter around the arc Fig. 20a. In contrast to this, the HTM process maintains the arc voltage low enough to shorten the arc length so as to create a buried arc, and as a result, the molten droplet transfer mode shifts from a globular transfer to a spray one Fig. 20b. This is probably because the buried arc causes the electrode wire to generate an additional arc between its side surface and the groove face, and thus, the wire tip becomes sharper more easily, thereby making the droplet detachment easier. That is, in high-current CO_2 arc welding, spatter can be reduced

Fig. 20 Observation of droplet transfer. **a** Conventional CO_2 welding process. **b** HTM welding process

(a) Conventional CO_2 welding process, (b) HTM welding process.

Fig. 21 Bead appearance by HTM process

significantly with the welding parameters suitable for deeper penetration.

7.5.2 Excellent bead appearance

The performance needed for the T-electrode was specified to be able to dress the convex bead made by the L-electrode buried arc and to obtain low spatter, even with a long arc length. In order to realize such specified performance, flux-cored wire was determined to be appropriate, and its slag composition was adjusted in consideration of the mixing ratio with the L-electrode chemistry. Consequently, a glossy bead appearance was obtained as shown in Fig. 21.

8 Conclusions

(1) It was observed that porosity reduced with an increase in penetration depth (L_{Pene}). This was proposed to be due to formation of consistent discharging passage for vaporized gas. In order to reduce the porosity in the fillet welding of primer-coated steel plate, it was found that the following measures are effective: (1) increasing the penetration depth (L_{Pene}) and (2) decreasing the non-penetrated joint root (L_{Root}).

(2) It was observed that porosity reduced with a decrease in non-penetration joint root (L_{Root}). This was proposed to be due to reduction in the source of gas vaporization in the fillet joint root.

(3) The probable reason for the phenomenon mentioned in item 2 above could be verified by observing directly the interior of the weld pool by using an X-ray video camera.

(4) To obtain the above conditions, it was effective to reduce the L-electrode torch angle and to use a high-current low-voltage welding condition for creating a buried arc.

(5) Even when CO_2 arc welding is used with solid wire, it has been found that the droplet transfer mode can be changed from a globular to a spray transfer by maintaining the arc voltage lower for shortening the arc length enough to create a buried arc.

(6) The hybrid tandem CO_2 arc welding process enables the achievement of both a larger L_{Pene} and a smaller L_{Root}, thereby preventing the occurrence of porosity. Though it is a high-current CO_2 arc welding process, ultra-low spatter performance can be achieved by creating a buried arc. Also, with the optimized wire chemistry, the bead appearance and shape are excellent.

References

1. Kamata (1993) Primer paint varieties vs. porosity resistance. J Jpn Weld Soc 62:507
2. Kamata et al (1991) Development of a flux-cored wire for inorganic-zinc-primer painted steel plates. Prepr Natl Meet Jpn Weld Soc 48:78
3. Maki et al (1988) Development of a flux-cored wire for wash-primer painted steel plates. Prepr Natl Meet Jpn Weld Soc 43:234
4. Kurokawa (2000) Past and present developments in flux-cored wire for MAG welding. Kobe Steel Eng Rep 50(3):74–77
5. Izutani et al (2012) Blowholes reduction in GMAW of galvanized steel sheet: part 1. Prepr Natl Meet Jpn Weld Soc 90:92
6. Nakamura et al (2012) Blowholes reduction in GMAW of galvanized steel sheet: part 2. Prepr Natl Meet Jpn Weld Soc 90:94
7. Izutani et al New welding process suitable for galvanized steel in the automotive industry, "J-Solution[TM] Zn," Kobe Steel Eng Rep 63:(1):54-59
8. Yuan et al (2012) Development of deep penetration & low spatter hybrid tandem GMAW process (part 1). Prepr Natl Meet Jpn Weld Soc 90:8–9
9. Yuan et al (2013) Development of deep penetration & low spatter hybrid tandem GMAW process (part 2). Prepr Natl Meet Jpn Weld Soc 92:16–17
10. Yuan et al (2014) Development of deep penetration & low spatter hybrid tandem GMAW process (part 3: porosity resistance). Prepr Natl Meet Jpn Weld Soc 94:124–125